NeuroImage 202 (2019) 116069

Contents lists available at ScienceDirect

NeuroImage

journal homepage: www.elsevier.com/locate/neuroimage

# Age-related differences in brain activations during spatial memory formation in a well-learned virtual Morris water maze (vMWM) task

Nadjalisse C. Reynolds [a], Jimmy Y. Zhong [b], Cherita A. Clendinen [b], Scott D. Moffat [b], Kathy R. Magnusson [a,*]

[a] Dept Biomedical Sciences, College of Veterinary Medicine & Linus Pauling Institute, Oregon State University, Corvallis, OR, 97331, USA
[b] School of Psychology, College of Sciences, Georgia Institute of Technology, Atlanta, GA, 30332, USA

ARTICLE INFO

*Keywords:*
Spatial memory
fMRI
Executive function
Prefrontal cortex
Neural compensation

ABSTRACT

The current study applied a rodent-based virtual Morris water maze (vMWM) protocol to an investigation of differences in search performance and brain activations between young and older male human adults. All participants completed in-lab practice and testing before performing the task in the fMRI scanner. Behavioral performance during fMRI scanning – measured in terms of corrected cumulative proximity (CCProx) to the goal – showed that a subgroup of older good performers attained comparable levels of search accuracy to the young while another subgroup of older poor performers exhibited consistently lower levels of search accuracy than both older good performers and the young. With regard to brain activations, young adults exhibited greater activations in the cerebellum and cuneus than all older adults, as well as older poor performers. Older good performers exhibited higher activation than older poor performers in the orbitofrontal cortex (BA 10/11), as well as in the cuneus and cerebellum. Brain-behavior correlations further showed that activations in regions involved in visuomotor control (cerebellum, lingual gyrus) and egocentric spatial processing (premotor cortex, precuneus) correlated positively with search accuracy (i.e., closer proximity to goal) in all participants. Notably, activations in the anterior hippocampus correlated positively with search accuracy (CCProx inversed) in the young but not in the old. Taken together, these findings implicated the orbitofrontal cortex and the cerebellum as playing crucial roles in executive and visuospatial processing in older adults, supporting the proposal of an age-related compensatory shift in spatial memory functions away from the hippocampus toward the prefrontal cortex.

## 1. Introduction

Age-related decline in spatial memory has been investigated using the Morris water maze (MWM), which was originally designed to assess place navigation in rodents (Morris, 1981, 1984; Sutherland and Dyck, 1984). Since its inception, the MWM has been refined by numerous researchers for assessing age-related decline in spatial memory in both rodents (see, e.g., Driscoll et al., 2006; Gallagher and Pelleymounter, 1988; Gallagher et al., 1993; Magnusson et al., 2007) and humans (see, e.g., Driscoll et al., 2003, 2005; Daugherty et al., 2015; Korthauer et al., 2016; Moffat and Resnick, 2002; Moffat et al., 2006, 2007; Zhong et al., 2017). The MWM is well-suited for investigating and comparing age-related changes in spatial memory across species (Astur et al., 2002) in view of substantial evidence showing that spatial memory formation is contingent on hippocampus-dependent processes in both humans (e.g., Antonova et al., 2009; Daugherty et al., 2015; Driscoll et al., 2003; Korthauer et al., 2016; Lester et al., 2017; Moffat et al., 2006) and rodents (e.g., Barnes et al., 2000; Chen et al., 2000; Clark et al., 1992; Driscoll et al., 2006, 2008; Magnusson, 1998; van Praag et al., 2005).

To facilitate a cross-species understanding of the cognitive and neural mechanisms underlying age-related decline in spatial memory, the current study employed a virtual MWM (vMWM), recently designed by Zhong et al. (2017), that closely matched the rodent-based MWM protocols of Magnusson and colleagues (see Magnusson, 1998, 2001; Magnusson et al., 2007; Zhao et al., 2009). Specifically, the structural properties of this vMWM closely resembled Magnusson et al.'s MWM with reference to spatial scale, and the types and locations of object cues. It was also distinct from other vMWMs with respect to the dynamic recording of *cumulative proximity to the goal*, a measure that offers a sensitive and reliable indicator of individual differences in spatial learning among aged animals (Gallagher et al., 1993; Maei et al., 2009; Zhong et al., 2017). A participant's proximity to the goal was computed

* Corresponding author. 307 Linus Pauling Science Center, Oregon State University, Corvallis, OR, 97331, USA.
*E-mail address:* kathy.magnusson@oregonstate.edu (K.R. Magnusson).

https://doi.org/10.1016/j.neuroimage.2019.116069
Received 14 May 2019; Received in revised form 3 July 2019; Accepted 2 August 2019
Available online 2 August 2019

every 200 ms for the duration of each trial, and the sum of these distances was corrected by deducting the cumulative proximity of an "ideal" path to the goal from the entry point. This "ideal" path reflected the shortest cumulative Euclidean distance between an entry point and the escape platform (see Zhong et al., 2017, for details of its computation).

In the extant neuroimaging literature, many studies have highlighted the structural and functional contributions of the hippocampus and navigationally-relevant extrahippocampal regions to search performance among the young and older adults (e.g., Antonova et al., 2011; Daugherty and Raz, 2017; Driscoll et al., 2003; Korthauer et al., 2016; Moffat et al., 2007; Yuan et al., 2014). Young adults have been shown to rely more on the hippocampal formation for accurate search performance in an analog of the vMWM, demonstrating higher bilateral activation in the hippocampus than older adults when encoding the goal location (Antonova et al., 2011). Compared with older adults, younger adults also possessed larger hippocampal volumes that contributed to higher levels of vMWM search accuracy (Driscoll et al., 2003; Moffat et al., 2007; Yuan et al., 2014). By contrast, poorer MWM search accuracy in older adults was accompanied by volumetric reductions in the hippocampus (Driscoll et al., 2003), prefrontal cortex (Antonova et al., 2011; Korthauer et al., 2016; Moffat et al., 2007), cerebellum, and caudate nucleus (Daugherty and Raz, 2017; Moffat et al., 2007).

When navigating a virtual maze and encoding its spatial layout, Moffat et al. (2006) further showed that older adults exhibited higher activations in the anterior cingulate gyrus and medial prefrontal cortex, but lower activation in the hippocampal formation, when compared with younger adults. Among older adults, the greater relevance of extrahippocampal regions to spatial memory formation resonates with the view that a compensatory shift in spatial memory performance – away from a central dependence on the hippocampus towards an increased engagement of frontal regions/systems – occurs with increasing age (Moffat et al., 2006; Zhong and Moffat, 2018).

Taking a cross-species or translational perspective, there were also findings from mice showing that age-related deficits in spatial memory formation were related to alterations in N-methyl-D-aspartate (NMDA) receptor binding and subunit expression in the frontal cortex (Das and Magnusson, 2008, 2011; Magnusson, 2001; Magnusson et al., 2007; Zamzow et al., 2016, 2019). Specially, manipulations of NMDA receptor subunits in the orbitofrontal cortices of mice affected spatial memory performance in the MWM (Brim et al., 2013; Das et al., 2012).

To our knowledge, there has been no prior vMWM-related findings showing whether an age-related shift in functional brain activity toward the frontal regions represents an adaptive mechanism for coping with age-related decline in hippocampus-dependent memory functions (Zhong and Moffat, 2018) or an age-related dedifferentiation of specialized neural mechanisms (Cabeza, 2001; Grady et al., 1994; Reuter-Lorenz and Cappell, 2008). Therefore, this study, through the comparison of different age/performance groups in a vMWM, aimed to investigate the different functions of extrahippocampal regions in spatial memory formation in both young and older adults, with focus on age and performance-related differences in prefrontal activity. This emphasis on the prefrontal cortex was informed by a recent review of the extant literature comparing the spatial navigational abilities of young and older adults (Zhong and Moffat, 2018), which highlighted the involvement of the prefrontal cortex as a key region in mediating a wide range of navigationally-relevant executive functions in both young and older adults.

## 2. Methods

### 2.1. Participants and cognitive assessment

21 young [age range: 18–30, *M* (*SD*) = 22.29 (3.31)] and 21 older human adults [age range: 60–79, *M* (*SD*) = 65.71 (4.51)] were recruited for this study. All participants were male due to the use of male subjects in the rodent-based protocols of Magnusson and colleagues (Magnusson, 1998, 2001; Magnusson et al., 2007; Zhao et al., 2009) and because sex differences in human vMWM performance have been observed in previous studies (e.g., Astur et al., 1998; Daugherty et al., 2015; Driscoll et al., 2003; Nowak et al., 2014, as cited by Zhong et al., 2017). Young adults were recruited from the psychology research volunteer pool at Georgia Institute of Technology and from the academic community in Atlanta, GA. Older adults were recruited from the greater Atlanta area using newspaper advertisements and notices posted at adult community centers. The study was approved by the Georgia Institute of Technology Institutional Review Board, and written informed consent was obtained from each participant.

Participants were tested individually, from the first to the 40-s (last) participant. The testing of young participants was interleaved with that of older participants, following a randomized sequence that was established and followed with consideration given to participants' availability. All participants were right-handed as assessed by the Edinburgh handedness questionnaire (Oldfield, 1971). Based on self-reported medical history, none of the participants were found to have a current diagnosis or history of coronary heart disease, stroke, diabetes, high blood pressure, and/or dementia. They were also negative with respect to any history of neurological and psychiatric illness and were not currently taking any neuro/psychoactive medications. Participants completed the Mini-Mental State Examination (MMSE; Folstein et al., 1975) with an inclusion score of 27 or higher required for participation (O'Bryant et al., 2008). They also completed the Center for Epidemiologic Studies Depression Scale (CES-D; Radloff, 1977), scoring below the suggested cutoff of 16. No one was excluded based on the MMSE and CES-D cutoff scores from the total sample of 42 participants. Participants had at least 20/40 visual acuity, normal color vision as judged from the Ishihara Color Plates Test, and normal contrast sensitivity based on the Mars Letter Contrast Sensitivity Test. Table 1 presents the details of comparisons of demographic and pretest measures between the two age groups.

### 2.2. Procedure

#### 2.2.1. Joystick control assessment

To ensure that all participants were comfortable with using an fMRI-compatible joystick for navigating the vMWM, they performed joystick practice and test, as described previously (see procedure of Zhong et al., 2017, for details) before starting the experiment proper. Both young and older participants were first instructed to use the joystick to guide themselves to four different objects (car, bench, tree, chairs) in a virtual arena before undergoing a joystick "speed test." This test required them to handle the joystick in moving through a long winding corridor within 2 min, in order to demonstrate an acceptable level of joystick control. On average, young and older adults completed the joystick task in around 1 min, with the young being comparatively faster (see Table 1).

#### 2.2.2. In-lab vMWM practice and testing

The vMWMs for both practice and testing purposes were designed using SketchUp Pro 2014 (Trimble Navigation Ltd., Sunnyvale, CA) and Unity Pro v5.0.2 (Unity Technologies, Inc., San Francisco, CA). Following joystick assessment, the participants remained seated in front of the same computer and practiced finding a round platform hidden beneath the water surface in a circular virtual pool (diameter = 16.0 virtual meters). Four object cues (soccer ball, cube, cylinder, tree) were positioned equidistant from each other on the deck of the pool and the hidden platform (diameter = 3.5 virtual meters) was positioned in the southeastern quadrant of the pool location. The participants searched for the platform over repeated trials from the same entry point in the northwest quadrant of the pool. The experimenter allowed each participant to practice as many trials as possible until he could find the hidden platform with ease (see Table 1, for no. of attempts per age group).

Upon practice completion, the participants continued to complete 24 place/hidden trials in a test environment that required them to find the hidden platform (see Fig. 1A), followed by six control/visible trials in a

**Table 1**
Descriptive statistics of demographic and pretest variables of young and older adults.

| Demographic/pretest variable | Young ($n = 21$) | | | Old ($n = 21$) | | | Difference (Old – Young) | | |
|---|---|---|---|---|---|---|---|---|---|
| | $M \pm SD$ | Min. | Max. | $M \pm SD$ | Min. | Max. | $M \pm SE$ | $t$ (40) | $p$-value |
| * Age | 22.29 ± 3.13 | 18 | 30 | 65.71 ± 4.51 | 60 | 79 | 43.43 ± 1.20 | 36.26 | <.001 |
| Education | 14.86 ± 1.31 | 12 | 17 | 15.43 ± 2.18 | 12 | 18 | 0.57 ± 0.56 | 1.03 | .311 |
| MMSE | 29.62 ± 0.59 | 28 | 30 | 29.19 ± 0.87 | 28 | 30 | −0.43 ± 0.23 | −1.87 | .068 |
| CES-D score | 5.38 ± 3.64 | 0 | 14 | 4.71 ± 4.22 | 0 | 13 | −0.67 ± 1.22 | −0.55 | .587 |
| Ishihara color blindness | 13.52 ± 2.18 | 4 | 14 | 14.00 ± 0.00 | 14 | 14 | 0.48 ± 0.48 | 1.00 | .323 |
| * Mars contrast sensitivity | 1.83 ± 0.07 | 1.72 | 2.00 | 1.72 ± 0.08 | 1.48 | 1.80 | −0.10 ± 0.02 | −4.49 | <.001 |
| * Speed test (s) | 56.57 ± 4.73 | 48 | 73 | 63.90 ± 15.30 | 50 | 120 | 7.33 ± 1.06 | 2.13 | .040 |
| No. of attempts in practice vMWM | 2.86 ± 1.06 | 1 | 5 | 3.57 ± 1.29 | 2 | 6 | 0.71 ± 0.36 | 1.96 | .057 |

*Note*. Min. = minimum; Max. = maximum; Education = education of participant in years; MMSE = Mini-Mental State Examination; CES-D = Center for Epidemiological Studies Depression scale; No. = number; vMWM = virtual Morris water maze. Asterisks indicate significant age group differences ($ps < 0.05$). The same statistics were reported previously by Zhong et al. (2017). Note that the Mars contrast sensitivity scores fell within the normal range for healthy older adults.

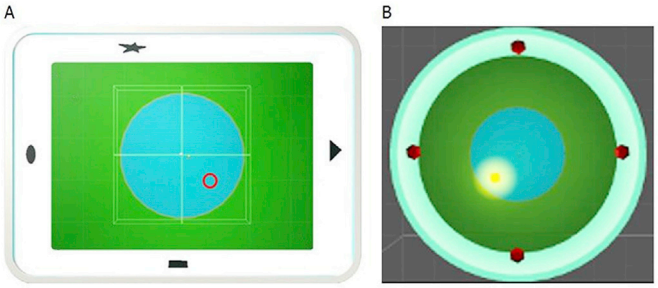


**Fig. 1.** Overhead views of (A) the vMWM arena used for hidden and probe trials and (B) the arena used for visible/control trials. (A) Four geometric objects were placed high up on the wall. The location of the platform in the southeastern quadrant is indicated by a red annulus (invisible to the participant). (B) Four identical red diamonds were placed on the rounded walls equidistant from each other to ensure that none of them would stand out as a distinctive positional cue. Participants navigated to the visible platform illuminated by a yellow halo [Source: Fig. 1 from Zhong et al. (2017). Reproduced with permission.].

control environment that required them to move directly to the visible platform (see Fig. 1B). The participants began each trial from varying entry positions. The location of the hidden platform was fixed in all place trials (Fig. 1A) while the location of the visible platform varied between the four quadrants of the pool across the control trials (see Zhong et al., 2017, for specific details regarding the physical attributes of these two vMWMs and the trial sequence). Critically, in the test environment, the participants were *not* informed that the hidden platform was kept stationary across all place trials. This was done to ensure a direct emulation of the testing conditions of Magnusson et al.'s rodent-based protocols (Zhong et al., 2017). Overall, this initial set of 33 experimental trials served to train participants to become familiar with the demands of hidden platform search before proceeding with the fMRI scan. For behavioral results derived from these trials, the reader is advised to refer to Zhong et al. (2017).

We used corrected cumulative proximity (CCProx) as the primary measure of vMWM search performance in all trials. This measure has been previously found to be a more sensitive measure of performance than the traditional latency or path length measures (see Gallagher et al., 1993; Maei et al., 2009). In brief, CCProx reflects the sum of the participant's Euclidean distances to the platform's center computed every 200 ms until the hidden platform was found (or when the time limit was reached) *corrected* for changes in the initial Euclidean distances away from the hidden platform from varying entry positions (see Zhong et al., 2017, for details of CCProx data recording).

### 2.2.3. fMRI preparation and testing

After completing in-lab practice and testing, the participants proceeded to complete four place and six visible trials (arranged in a randomized/interleaved sequence) in a mock fMRI scanner (MRI Simulator, Psychology Software Tools, Sharpsburg, PA). This exposed the participants to the confined space during fMRI scanning and ensured that they were comfortable with handling the fMRI-compatible joystick while lying in a supine position. Importantly, at the beginning of the mock scanner trials, the participants were told that they would be exposed to the same test environments as they experienced in the lab and that the hidden platform would remain stationary in all place trials. These instructions were intended to ensure that all participants were kept aware of the static nature of the hidden platform and that they would engage memory-related processes, as much as possible, when performing the vMWM task in the scanner. After completing all trials in the mock scanner, the participants entered the actual MRI scanner and completed 16 place and eight control trials arranged in a randomized/interleaved sequence. The maximum time durations in both place and control trials in the mock and actual fMRI scanners were kept identical at 30 s (see Fig. 2). The intertrial interval was set at 5.0 s for both trial types (see Fig. 2, panels C and F). All trials in the fMRI scanner were completed in one functional run that lasted not more than a maximum duration of 10 min.

### 2.2.4. fMRI image acquisition and statistical analysis

Brain images were collected at the Georgia State/Georgia Tech Center for Advanced Brain Imaging on a 3 T S TIM Trio magnetic Resonance Imaging system (Siemens Medical Solutions, Erlangen, Germany) with a 12-channel head coil. Whole-brain structural images were collected in the sagittal plane using a T1-weighted high-resolution magnetization-prepared rapid gradient-echo (MP-RAGE) sequence (TR = 2250 ms, TE = 4.18 ms, TI = 900 ms, field of view = 256 mm, voxel size = 1.0 mm × 1.0 mm x 1.0 mm, flip angle = 9°, slice no. = 176, slice thickness = 1.00 mm). Whole-brain echo-planar imaging (EPI) with BOLD contrast was used to collect functional data in the transverse plane in 37 interleaved oblique slices (TR = 2000 ms, TE = 30 ms, field of view = 204 mm, voxel size = 3.0 mm × 3.0 mm x 3.0 mm, flip angle = 70°, slice thickness = 3.00 mm, 37 slices).

*2.2.4.1. Preprocessing of single-subject data.* fMRI data from all participants were processed and analyzed using the *Analysis of Functional Neuroimages (AFNI)* software package [National Institute of Mental Health, National Institutes of Health; available at: https://afni.nimh.nih.gov/download)]. The brain images/volumes were first corrected for slice timing and realigned to the first image. Motion correction then followed by registering the BOLD images to the average time-shifted image/volume in each run to correct for image distortions caused by susceptibility-by-movement interactions (Andersson et al., 2001). Fourier interpolation was applied to the heptic degree over two passes to reduce the voxel intensity differences between images. Subsequently, the high-resolution T1 structural image from each participant was co-registered to the mean slice timing and motion corrected BOLD image using AFNI's "align_epi_anat.py" script. These co-registered structural and BOLD

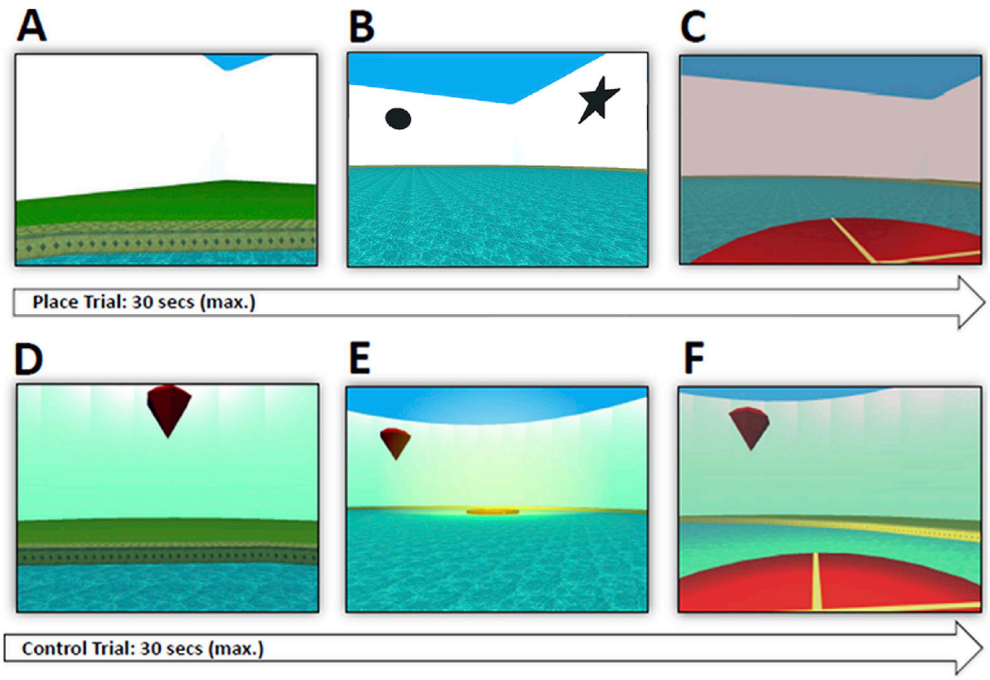


**Fig. 2.** Scenes of the vMWMs used for assessing place navigation (A–C) and visuomotor control (D–F) during mock and real fMRI scanning. (A–B) In the test environment, participants began each trial facing the wall of a circular pool and then used a joystick to explore the pool based on black-and-white shape cues located high up on the walls. (C) When the subject entered the invisible circular region that encapsulated the hidden platform location, it surfaced immediately, and the participant could rotate in place for 5.0 s. (D) The control environment featured the same pool as that of the test environment but without any distinctive object or geometric cues (e.g., no corners of the room or different objects). (E–F) Subjects navigated as quickly as possible to the visible platform illuminated by a yellow halo [Source: Fig. 2 from Zhong et al. (2017). Adapted and reproduced with permission.].

images were then spatially normalized into standard Montreal Neurological (MNI) space, and resampled during normalization to 2 $mm^3$ isotropic voxels, using AFNI's "@auto_tlrc" program. The structural images of old and young participants were averaged after normalization, respectively, to act as underlays for displaying overlays of functional images collected from each age group. For the display of overlays of functional data comparing the age groups, the structural images of all participants were averaged after normalization to act as the underlay. All mean structural images were resampled to 1 $mm^3$ isotropic voxels for a high-resolution display of the anatomical regions.

To identify task-related changes in the BOLD signal, the time courses of the place/hidden and control/visible trials were examined through a whole-brain analysis. The predicted hemodynamic response for each block of these two types of trials was modeled based on a duration modulated response function as part of AFNI's "3dDeconvolve" program. The slice timing and motion corrected data was smoothed with a 6.4 mm FWHM Gaussian kernel before convolution. Timing information about trial onsets and duration in both trial types/blocks was entered as task regressors into the general linear model. These two regressors were accompanied by six motion regressors-of-no-interest that registered noise pertaining to excessive head motion along the three axes/planes (xyz) of rotation and translation, respectively. A general linear test then subtracted the parameter estimates representing the control/visible condition from those representing the place/hidden condition to generate whole-brain contrast maps that conveyed the BOLD signal changes during hidden platform search. These difference values were converted to percent signal change (PSC) values to ensure standardized comparisons at the group level. These PSC values were corrected for any extraneous effect posed by the autocorrelation of temporal residuals from the regression models via AFNI's "3dREML" program.

*2.2.4.2. Group-level random effects analysis.* With the contrast maps from each participant, random effect analyses using AFNI's "3dttest++" program were conducted to examine changes in BOLD signals within each age group and between the age/performance groups. To control for individual differences in visuomotor control that could affect vMWM search performance, *mean visible path length* (the path length averaged across all control trials) was included as a covariate in these random effects models. This covariate conveyed a direct measure of the distance covered in reaching a visible target based on joystick deflections and has been successfully applied by Zhong et al. (2017) to the analysis of data from the in-lab testing phase. To correct for multiple comparisons of activated voxels across the entire brain/search volume, cluster thresholding was conducted using AFNI's "3dClustSim" program based on a 10,000 iteration Monte Carlo simulation analysis on voxels within the group-level functional brain space (234,177 voxels). AFNI's "3dFWHMx" program was used to compute the spatial autocorrelation function parameters (representing the smoothness of the time series noise from all participants) for generating random noise cluster fields spanning across the entire brain volume in the Monte Carlo simulation. Based on the analysis, the minimum number of voxels fulfilling a height/voxel-wise threshold of 0.01 and a cluster-level/extent threshold of 0.05 was determined to be 218. This cluster size threshold was used for all random effects analyses.

## 3. Results

### 3.1. Behavioral analysis

Older adults were separated into good-performing and poor-performing groups based on a median split of their mean CCProx values over the 16 place trials completed in the fMRI scanner. CCProx values from the place trials completed in the mock scanner were excluded because those trials were intended for practice only and not directed toward assessment and interpretation together with the fMRI results. This median split procedure has been successfully implemented with reference to the data acquired from the 24 place trials during the in-lab testing phase (see Zhong et al., 2017, for the rationale of this approach and earlier findings). The median CCProx value based on the mean CCProx values attained by the older adults was found to be 114.87 virtual m. Older adults with mean CCProx values higher and lower than this median value were categorized as poor and good performers respectively. This resulted in 11 good performers and 10 poor performers. Table 2 presents the details of comparisons of demographic and pretest variables between the two older subgroups.

#### 3.1.1. Place/hidden trials

A mixed-model ANCOVA was used to analyze performance of the

**Table 2**
Descriptive statistics of demographic and pretest variables of older good- and poor performers.

| Demographic or pretest variable | Older Good Performers ($n = 11$) | | | Older Poor Performers ($n = 10$) | | | Difference (Good Old – Poor Old) | | |
|---|---|---|---|---|---|---|---|---|---|
| | $M \pm SD$ | Min. | Max. | $M \pm SD$ | Min. | Max. | $M \pm SE$ | $t$ (19) | $p$-value |
| Age | 66.00 ± 3.52 | 60 | 70 | 65.40 ± 5.58 | 60 | 79 | 0.60 ± 2.02 | 0.30 | .769 |
| Education | 15.73 ± 2.28 | 12 | 18 | 15.10 ± 2.13 | 12 | 18 | 0.63 ± 0.97 | 0.65 | .521 |
| MMSE | 29.36 ± 0.81 | 28 | 30 | 29.00 ± 0.94 | 28 | 30 | 0.36 ± 0.38 | 0.94 | .357 |
| CES-D score | 5.36 ± 4.25 | 0 | 11 | 4.00 ± 4.29 | 0 | 13 | 1.36 ± 1.87 | 0.73 | .475 |
| Ishihara color blindness | 14.00 ± 0.00 | 14 | 14 | 14.00 ± 0.00 | 14 | 14 | | | |
| Mars contrast sensitivity | 1.74 ± 0.06 | 1.60 | 1.80 | 1.70 ± 0.09 | 1.48 | 1.80 | 0.04 ± 0.03 | 1.21 | .241 |
| Speed test (s) | 59.09 ± 4.28 | 55 | 70 | 69.20 ± 20.55 | 50 | 120 | −10.11 ± 6.33 | 1.60 | .127 |
| * No. of attempts in practice vMWM | 3.00 ± 0.77 | 2 | 4 | 4.20 ± 1.48 | 2 | 6 | −1.20 ± 0.51 | 2.36 | .028 |

*Note*. Min. = minimum; Max. = maximum; Education = education of participant in years; MMSE = Mini-Mental State Examination; CES-D = Center for Epidemiological Studies Depression scale; No. = number; vMWM = virtual Morris water maze. Asterisks indicate significant age group differences ($ps < 0.05$).

young and two older subgroups across four blocks of place trials completed in the fMRI scanner. Each block comprised four place trials. Mean visible path length over the eight control trials completed in the scanner (mean visible path length) was used as a covariate in the analysis of place trial blocks to adjust for age or performance-related differences in visuomotor control ability.

After controlling for the significant covariate effect of mean visible path length ($F$ (1, 38) = 13.82; $p = 0.001$; partial $\eta^2 = 0.267$), there were significant main effects of age/performance group ($F$ (2, 38) = 26.43; $p < .001$; partial $\eta^2 = 0.582$) and trial block ($F$ (3, 36) = 2.96; $p = 0.045$; partial $\eta^2 = 0.198$) [see Fig. 3]. The group x trial block interaction did not reach significance ($F$ (6, 74) = 0.58; $p = .747$; partial $\eta^2 = 0.045$). Post hoc Bonferroni pairwise comparisons showed that older poor performers exhibited higher CCProx values overall ($M \pm SE = 193.59 \pm 14.94$) than both older good performers ($M \pm SE = 85.85 \pm 12.44$) [$p < .001$] and younger adults ($M \pm SE = 57.70 \pm 9.34$) [$p < .001$].[1] By contrast, older good performers attained comparable performance as younger adults ($p = .220$). Older poor performers also stood out for not demonstrating any noticeable decline in CCProx across trial blocks.

### 3.1.2. Control/visible trials

A mixed-model ANOVA was used to analyze performance of the three age/performance groups across all eight control trials completed in the scanner. There were significant main effects of age/performance group ($F$ (2, 39) = 8.60; $p = 0.044$; partial $\eta^2 = 0.306$) and trial ($F$ (7, 33) = 38.75; $p < 0.001$; partial $\eta^2 = 0.892$) [see Fig. 3]. The group × trial interaction did not reach significance ($F$ (14, 68) = 1.19; partial $p = .301$; $\eta^2 = 0.197$). Similar to the place trial analysis, post hoc Bonferroni comparisons showed that older poor performers exhibited higher CCProx values overall ($M \pm SE = 61.48 \pm 6.46$) than both older good performers ($M \pm SE = 33.36 \pm 6.16$) [$p = .009$] and younger adults ($M \pm SE = 29.73 \pm 4.46$) [$p = 0.001$]. The trial effect primarily emanated from lower CCProx values attained by all age/performance groups on the third and eighth control trials, relative to the first trial ($ps < .010$). The relatively lower CCProx values attained on these trials were attributed to the visible platform being located at the center of the pool and within close proximity to the respective entry points.

### 3.1.3. Further examination of performance differences based on two subgroups of young performers

To examine whether *younger* good and poor performers would exhibit patterns of place and trial performance in comparison to the two subgroups of older performers, we conducted another median split based on the median CCProx value attained by all young participants (median = 34.81). 11 young adults scored below the median and were classified as good performers. 10 young adults scored above the median and were classified as poor performers.

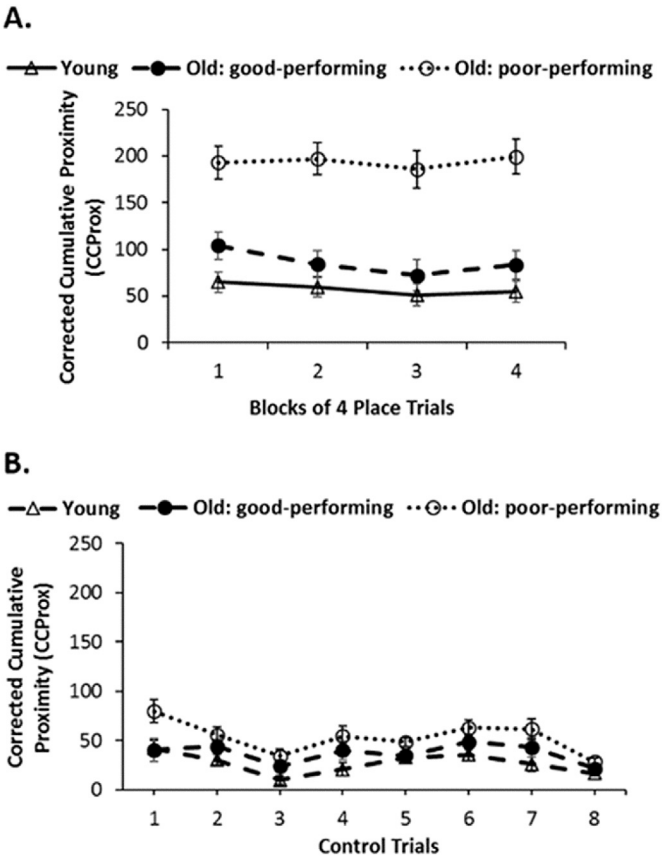


**Fig. 3.** Performance of young participants, older good performers, and older poor performers in the vMWM in place (A) and control (B) trials in the fMRI scanner. Means and standard errors (*SE*s) of place trial blocks were adjusted for the significant covariate effect of mean visible path length. The range of CCProx values along the vertical axis were kept identical in both panels to facilitate the comparison of values between trial types. Regardless of trial type, older poor performers were exceptional for exhibiting the highest CCProx values overall. Error bars depict ±1 *SE*.

When examining performance across the place trials, the same mixed-model ANCOVA was conducted with age/performance groups updated to four levels (younger good and poor performers versus older good and poor performers). The general pattern of results was similar to that found with three groups. After controlling for the significant covariate effect of mean visible path length ($F$ (1, 38) = 13.37; $p = 0.01$; partial $\eta^2 = 0.265$), There was a significant main effect of age/performance group ($F$ (3, 37) = 19.76; $p < .001$; partial $\eta^2 = 616$). The main effect of trial block approached significance ($F$ (3, 35) = 2.59; $p = 0.068$; partial $\eta^2 = 0.182$). The group × trial interaction did not reach significance ($F$ (9,

[1] Note that the descriptives reported for place trial performance in this subsection and subsection 3.1.3. were adjusted for the covariate effect of mean visible path length.

111) = 0.51; $p = .866$; partial $\eta^2 = 0.040$). Across all place trials, post hoc Bonferroni pairwise comparisons showed that both younger good ($M \pm SE = 42.27 \pm 12.46$) and poor performers ($M \pm SE = 73.79 \pm 12.71$) exhibited significantly lower CCProx values than older poor performers ($M \pm SE = 194.73 \pm 14.53$) [$ps < .001$ for both comparisons]. There were no significant performance differences between younger good and poor performers ($p = .473$), as well as between older good performers ($M \pm SE = 85.61 \pm 12.09$) and either group of young performers [$p = .092$ for the comparison involving younger good performers; $p = .100$ for the comparison involving younger poor performers].

Performance of the four age/performance groups across the control trials were also re-examined using the same mixed-model ANOVA used in the earlier analysis. Once more, the general pattern of results was similar to that found with three groups. There were significant main effects of age/performance group ($F$ (3, 38) = 5.73; $p = 0.002$; partial $\eta^2 = 0.311$) and trial ($F$ (7, 32) = 38.65; $p < 0.001$; partial $\eta^2 = 0.894$). The group × trial interaction did not reach significance ($F$ (21, 102) = 0.93; $p = .556$; partial $\eta^2 = 0.161$).). Across all control trials, post hoc Bonferroni pairwise comparisons showed that both younger good ($M \pm SE = 27.42 \pm 6.22$) and poor performers ($M \pm SE = 32.26 \pm 6.52$) exhibited significantly lower CCProx values than older poor performers ($M \pm SE = 61.48 \pm 6.46$) [$p = .003$ for the comparison involving younger good performers; $p = .018$ for the comparison involving younger poor performers]. There were no significant performance differences between younger good and poor performers ($p = .100$), as well as between older good performers ($M \pm SE = 33.36 \pm 6.16$) and either group of young performers [$ps = .100$ for both comparisons].

Overall, in view that the median split of the young adults did not yield any between-subjects differences that deviated from the initial findings obtained from three age/performance groups, we kept all young participants in one group and conducted all subsequent fMRI analyses without any subcategorization of the young adults. We also did this to increase statistical power for between-group comparisons.

### 3.2. Brain activations in young and older adults

Brain activation patterns were first examined in young and older participants with place trial activations contrasted against control trial activations ([place > control], see Table 3). In the analysis of brain activations within each age/performance group, the PSC values derived from the contrast were tested for significance based on a one-sample $t$-test that controlled for the covariate effect of mean visible path length within that group. One older adult – categorized as a poor performer – was excluded from analysis due to excessive head motion.

As shown on Table 3 and Fig. 4, we found significant clusters of activations in both age groups in the left middle frontal gyrus (BA 6 in young; BA 9/10 in old), bilateral inferior frontal gyrus (BA 47), and right cuneus (BA 18). Both groups also exhibited unilateral activations in the superior occipital gyrus (BA 19; left in young, right in old). As for age group-specific activations, young adults exhibited activations in the posterior cerebellum and caudate, whereas older adults exhibited activations in the posterior cingulate gyrus (BA 31). We further examined the activation patterns separately for older good and poor performers. As shown in Table 4, both performance groups exhibited relatively distinctive regions of activations, with older good performers having more significant clusters of activations. Older good performers exhibited widespread activations in the fronto-parietal network encompassing the dorsolateral (BA 9) and orbitofrontal prefrontal cortices (BA 10), the inferior parietal lobule (BA 40), and the precuneus (BA 19), whereas older poor performers exhibited activations over a smaller range of regions encompassing the middle frontal gyrus (BA 9), the precuneus (BA 31), and the posterior cerebellum.

To investigate differences in underlying spatial memory-related brain response between the age/performance groups, differences in brain activations between young, good-performing older, and poor-performing older adults were assessed with respect to the [place > control] contrast. These differences in brain activations were adjusted for the significant covariate effect of mean visible path length. Group comparisons were performed between the young and all older adults categorized as a single group, as well as divided between good and poor performers. Table 5 shows the regions with significant clusters of activations.

**Table 3**
Activations in young and old adults.

| Region | Side | BA | Cluster size (voxels) | x | y | z | T-value |
|---|---|---|---|---|---|---|---|
| *Young* ($n = 21$) | | | | | | | |
| Superior occipital gyrus | L | 19 | 9093 | −32 | −84 | 30 | 8.85 |
| Cerebellum (posterior lobe) | L | | 5290 | −14 | −42 | −42 | 6.61 |
| Middle frontal gyrus | R | 6 | 2266 | 26 | 0 | 54 | 7.37 |
| | L | 6 | 1038 | −36 | −2 | 52 | 6.31 |
| Medial frontal gyrus | R | 8 | 494 | 10 | 18 | 50 | 4.30 |
| Inferior frontal gyrus | R | 47 | 967 | 36 | 28 | 0 | 8.39 |
| | L | 47 | 710 | −30 | 30 | 0 | 7.42 |
| Cuneus | R | 18 | 475 | 14 | −98 | 14 | 6.52 |
| Caudate head | R | | 320 | 10 | 6 | 2 | 4.98 |
| *Old* ($n = 20$) | | | | | | | |
| Posterior cingulate | R | 31 | 5370 | 20 | −58 | 24 | 8.04 |
| Inferior frontal gyrus | R | 47 | 3196 | 34 | 30 | 0 | 6.95 |
| | L | 47 | 956 | −32 | 28 | 2 | 7.48 |
| Middle frontal gyrus | L | 9 | 2910 | −46 | 32 | 28 | 7.70 |
| | L | 10 | 340 | −38 | 58 | 8 | 5.57 |
| Superior occipital gyrus | R | 19 | 389 | 34 | −82 | 30 | 5.27 |
| Cuneus | R | 18 | 222 | 10 | −88 | 20 | 4.39 |

*Note.* R = Right, L = Left. For activations within the same region, the larger cluster is shown first.

Young adults exhibited greater activations than all older adults as a single group, as well as the poor-performing older subgroup, in the cuneus (BA 18) and anterior cerebellum (see Fig. 5A). Compared with older good performers, young adults exhibited greater activation in the anterior cerebellum only (see Fig. 5B). Between the two older subgroups, older good performers exhibited greater activations than older poor performers in the anterior prefrontal/orbitofrontal cortex (BA 10/11) and cuneus (BA 18) [see Fig. 5C].

### 3.3. Relating brain activations to vMWM search accuracy

In addition to the within- and between-group analyses, we performed regressions between brain activation patterns – from all participants, young, and older adults, respectively – and an inverse mean CCProx measure that provided an approximate measure of search accuracy across all place trials. Inverse CCProx was computed so that higher search accuracy values represented better performance.

In all correlational analyses, the height threshold was set at .01 with the extent-level threshold remaining at 218. The findings are shown in Table 6. With all participants involved, higher search accuracy was associated with increased activation in the middle frontal gyrus/premotor cortex (BA 6), lingual gyrus (BA 18), precuneus (BA7), and posterior cerebellum. Among young participants, higher search accuracy was associated with increased activation in the posterior cerebellum, anterior hippocampus (within the dorsal layers/region and close to entorhinal area BA 28), inferior temporal gyrus (BA 20/37), and middle frontal gyrus/frontal eye fields (BA 8). Among older adults, higher search accuracy was associated with increased activation in only one region – the right precentral gyrus (BA 6), proximal to the premotor cortex, though at a subthreshold level. Further correlational analyses conducted on older good and poor performers respectively did not reveal any

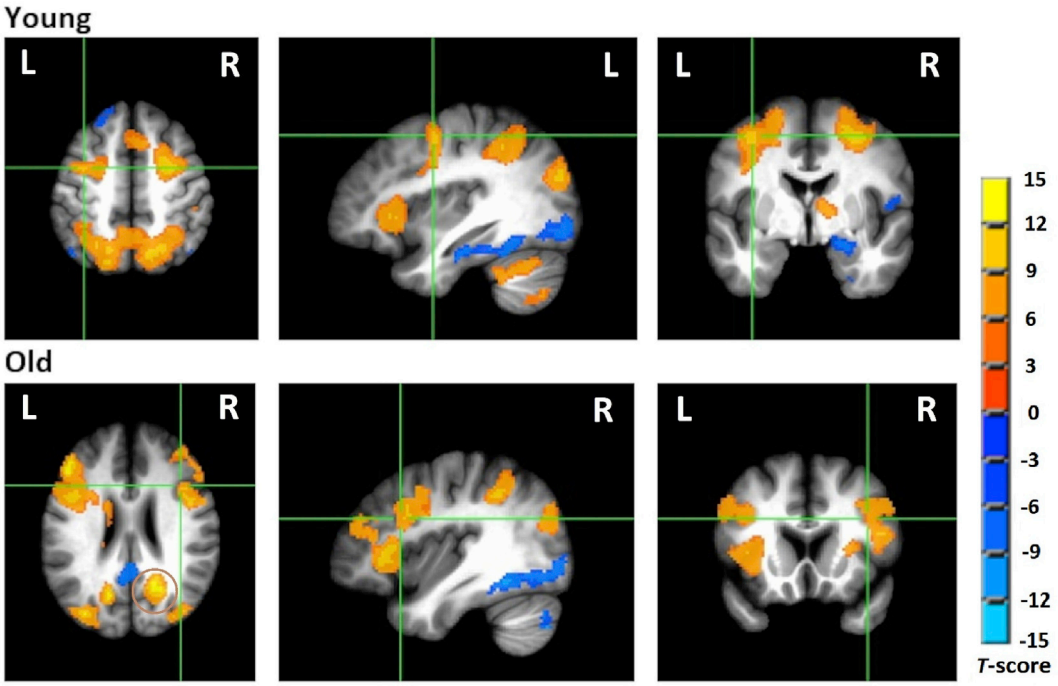


**Fig. 4.** Brain activations in young and older adults derived from the [place > control] contrast. Activation images in each age group are superimposed on spatially normalized high-resolution T1-weighted image averaged across all participants within that group. Both age groups exhibited large extents of activations in the frontal cortex. Young and old adults exhibited the highest degree of activation in the bilateral occipital cortex (top left panel), and right posterior cingulate (bottom left panel; circled in red), respectively. Images of whole-brain activations were taken with cross-hairs centered on the left premotor cortex (BA 6) in the young [x = −36, y = −2, z = 52] and on the right dorsolateral prefrontal cortex (BA 9) in the old [x = 39, y = 18, z = 27]. Cooler colors represent areas in the inferior occipital lobe (e.g., fusiform gyrus) with greater activation during the control trials than during the place trials (not reported). L = left hemisphere; R = right hemisphere.

**Table 4**
Activations in two subgroups of old adults.

| Region | Side | BA | Cluster size (voxels) | x | y | z | *T*-value |
|---|---|---|---|---|---|---|---|
| *Older good performers* ($n = 11$) | | | | | | | |
| Middle frontal gyrus | L | 9 | 1635 | −48 | 32 | 28 | 7.53 |
| | R | 9 | 443 | 46 | 8 | 30 | 7.09 |
| | R | 10 | 253 | 32 | 52 | 0 | 6.50 |
| Inferior parietal lobule | L | 40 | 654 | −42 | −44 | 48 | 6.21 |
| Inferior frontal gyrus | L | 47 | 534 | −30 | 32 | −2 | 6.58 |
| Superior parietal lobule | R | 7 | 474 | 32 | −60 | 48 | 7.23 |
| Medial frontal gyrus | R | 6 | 385 | 20 | 6 | 52 | 5.52 |
| Posterior cingulate | R | 31 | 345 | 16 | −58 | 18 | 6.01 |
| Precuneus | L | 19 | 313 | −32 | −82 | 34 | 6.79 |
| Superior occipital gyrus | R | 19 | 298 | 44 | −78 | 30 | 10.07 |
| *Older poor performers* ($n = 9$) | | | | | | | |
| Precuneus | R | 31 | 350 | 24 | −62 | 24 | 6.81 |
| | L | 31 | 223 | −14 | −58 | 26 | 8.99 |
| Cerebellum (posterior lobe) | L | | 272 | 44 | −68 | −22 | 15.29 |
| Middle frontal gyrus | R | 9 | 228 | 42 | 16 | 30 | 7.18 |

*Note*. R = Right, L = Left. For activations within the same region, the larger cluster is shown first.

**Table 5**
Between-group comparisons.

| Region | Side | BA | Cluster size (voxels) | x | y | z | *T*-value |
|---|---|---|---|---|---|---|---|
| *Young > Old* | | | | | | | |
| Cerebellum (anterior lobe) | R | | 1661 | 6 | −68 | −10 | 5.34 |
| Cuneus | R | 18 | 370 | 14 | −98 | 14 | 4.75 |
| Cerebellum (posterior lobe) | R | | 263 | 44 | −62 | −32 | 3.56 |
| *Young > Older good performers* | | | | | | | |
| Cerebellum (anterior lobe) | L | | 7364 | −2 | −60 | −4 | 4.59 |
| *Young > Older poor performers* | | | | | | | |
| Cerebellum (anterior lobe) | L | | 1839 | −4 | −44 | −16 | 6.10 |
| Cuneus | R | 18 | 402 | 14 | −98 | 14 | 4.35 |
| *Older good performers > Older poor performers* | | | | | | | |
| Middle frontal gyrus | L | 11 | 763 | −20 | 48 | −12 | 10.59 |
| Superior frontal gyrus | R | 10 | 262 | 24 | 58 | 4 | 6.65 |
| Cuneus | L | 18 | 243 | −2 | −100 | 6 | 5.22 |
| Cerebellum (posterior lobe) | R | | 229 | 14 | −88 | −30 | 6.31 |

*Note*. R = Right, L = Left. For activations in the same brain region, the larger cluster is shown first.

significant cluster of activation; no region correlated positively with search accuracy at a subthreshold level. Figs. 6 and 7 show a sample of the navigationally relevant regions that correlated with search accuracy in all participants and in each age group, respectively.

## 4. Discussion

The current study showed that a subgroup of poor-performing older adults – found previously by Zhong et al. (2017) – experienced challenges in forming spatial memories when compared with younger adults. Consistent with the earlier findings shown by Zhong et al. (2017), older poor performers exhibited significantly higher CCProx values (i.e., lower

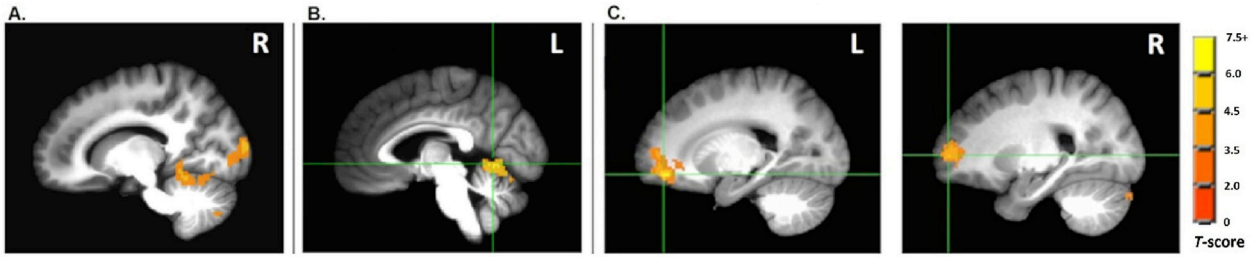


**Fig. 5.** Group comparisons of young, good-performing older, and poor-performing older adults during place trials compared with control trials. Activation images are superimposed on spatially normalized high-resolution T1-weighted image averaged across all participants. **(A)** Young adults exhibited higher activations than older poor performers in the cuneus (BA 18) and anterior cerebellum (both activations seen from the right hemisphere). **(B)** Young adults exhibited higher activations than older good performers in the anterior cerebellum only. **(C)** Older good performers exhibited higher activations than older poor performers in the middle frontal gyrus (BA 11; left in panel) and superior frontal gyrus (BA 10; right in panel). L = left hemisphere; R = right hemisphere.

**Table 6**
Positive correlations with search accuracy.

| Region | Side | BA | Cluster size (voxels) | X | y | z | *T*-value |
|---|---|---|---|---|---|---|---|
| *All participants* | | | | | | | |
| Lingual gyrus | L | 18 | 964 | −8 | −90 | −10 | 4.37 |
| Precuneus | R | 7 | 539 | 16 | −66 | 52 | 4.48 |
| Cerebellum (posterior lobe) | L | | 436 | −12 | −74 | −46 | 3.66 |
| Middle frontal gyrus | R | 6 | 237 | 30 | −4 | 46 | 4.63 |
| *Young* | | | | | | | |
| Cerebellum (posterior lobe) | L | | 1507 | −38 | −58 | −44 | 5.39 |
| Hippocampus | R | | 427 | 26 | −18 | −10 | 5.23 |
| Inferior temporal gyrus | R | 20/37 | 277 | 46 | −18 | −28 | 4.39 |
| Middle frontal gyrus | L | 8 | 227 | −36 | 32 | 42 | 4.10 |
| *Old* [a] | | | | | | | |
| Precentral gyrus | R | 6 | 60 | 39 | −8 | 36 | 4.67 |

*Note*. R = Right, L = Left. For activations in the same brain region, the larger cluster is shown first.

[a] Brain-behavior correlation among older adults occurred in only one region at the subthreshold cluster size of 60.

search accuracy) than both the young and older good performers across all place trial blocks. We interpreted these group differences in the context of corresponding differences in hippocampal and extra-hippocampal patterns of brain activation in each group.

Starting with an examination of prefrontal activity, we found prominent prefrontal activations in all age/performance groups, encompassing BA 6/8 in young, BA 9/10 in old and BA47 in both age groups. Collectively, these regions have been shown by previous studies to be important for mediating goal-directed processes during spatial navigation in both young and older adults (Zhong and Moffat, 2018). For example, activations in the mPFC (BA 9/10) have been shown to be related to imagining the location of a goal location and planning out the best route to reach it (Spiers and Maguire, 2006, 2007), while activations in the ventromedial prefrontal cortex have been proposed to be pertinent for monitoring changing directions toward a goal location and suppressing the processing of any irrelevant stimuli (Spiers, 2008). Between-group analysis showed that relatively higher prefrontal activations were found only in the comparison between older good and poor performers. Specifically, older good performers exhibited greater activations than older poor performers in two anterior prefrontal regions (BA 10, BA 11) that constitute the central components of the orbitofrontal cortex (OFC) (Frey and Petrides, 2000; Kringelbach and Rolls, 2004; Ongür et al., 2003; Ramnani and Owen, 2004). Most probably, older good performers' higher engagement of these orbitofrontal regions facilitated the processing of visuospatial stimuli associated with goal-directed navigation. This interpretation gains support from previous studies that showed a preferential involvement of the orbitofrontal cortex (BA 10/11) in judging inter-item spatial relationships (Slotnick and Moo, 2006), as well as in selecting or initiating actions on the basis of external cues, anticipated rewards (Domenech and Koechlin, 2015), and spontaneous decisions (Zhong, 2016). In view of these previous findings, it is most likely that older good performers' higher orbitofrontal activations (as compared with older poor performers) represented a heightened awareness of visuospatial cues and their underlying relationships when making goal-directed decisions and actions.

Furthermore, older good performers' bilateral activation of the dorsolateral prefrontal cortex (dlPFC) [BA 9], along with activations in posterior regions such as the posterior cingulate cortex and the precuneus, suggest engagement in the processing of goal-relevant stimuli/cues. This interpretation aligns well with previous studies that demonstrate the involvement of the dorsolateral cortex in associative/relational information processing in working memory (see, e.g., Blumenfeld et al., 2011; Curtis and D'Esposito, 2004; see also Funahashi, 2017, for a review) and the pertinence of the posterior cingulate cortex (usually comprising the retrosplenial cortex) and precuneus for mediating the organization and transformation of spatial information/representations

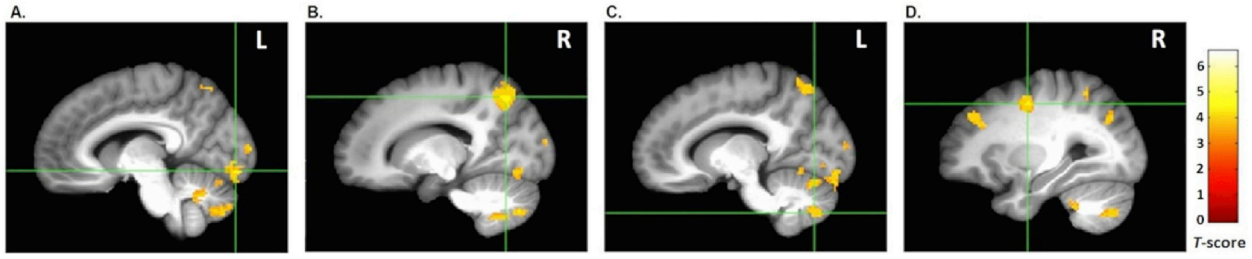


**Fig. 6.** Brain-behavior correlations showing the positive relationships between search accuracy and whole brain activation patterns in all participants. Activation images are superimposed on spatially normalized high-resolution T1-weighted image averaged across all participants. Higher search accuracy (i.e., lower mean CCProx) was associated with increased activation in the (A) lingual gyrus (BA 18), (B) precuneus (BA 7), (C) posterior cerebellum, and (D) middle frontal gyrus/premotor cortex (BA 6). Cross hairs were centered on the peak voxel of activation in each specified region. L = left hemisphere; R = right hemisphere.

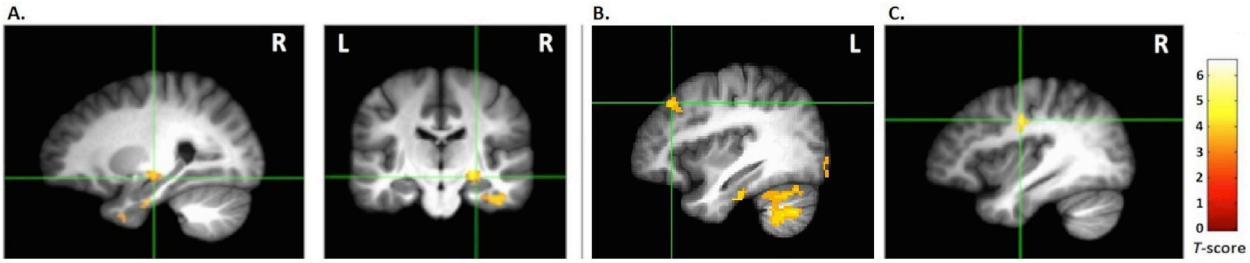


**Fig. 7.** Brain-behavior correlations showing the positive correlations between search accuracy and whole brain activation patterns in young and older participants respectively. Activation images in each age group are superimposed on spatially normalized high-resolution T1-weighted image averaged across all participants within that group. Among the young, higher search accuracy was associated with increased activation in the (A) anterior hippocampus (both sagittal and coronal views are shown) and (B) middle frontal gyrus/frontal eye fields (BA 8). Among the old, higher accuracy was associated with increased activation in the (C) precentral gyrus at a subthreshold level. Cross hairs were centered on the peak voxel of activation in each specified region. L = left hemisphere; R = right hemisphere.

(see, e.g., Chrastil et al., 2017; Gramann, 2013; Gramann et al., 2010; Iaria et al., 2007; Shine et al., 2016). Specifically, activations in the posterior cingulate cortex and the precuneus might reflect older good performers' attention to relevant visuospatial stimuli/cues and corresponding activation in the dlPFC might have facilitated the associative learning or "binding" of these pieces of information for successful goal search. For example, effective associative learning might take the form of realizing that two geometric cues (the triangle and square) could function as proximal markers/associates of the hidden platform's location. By contrast, the absence of bilateral activation in the dlPFC – as well as in the orbitofrontal cortex (BA 10/11) – among older poor performers might explain why they were generally unsuccessful/inaccurate at finding the hidden platform. Most probably, the relatively low level of prefrontal activations in older poor performers may adversely affect their perception of spatial cues and relationships, and associations between object cues, goal location, and any goal-related responses.

In addition to all these prefrontal activations, the findings showed that the cerebellum was commonly activated in all between-group comparisons. Young adults exhibited greater activation in the anterior cerebellum than either group of older performers, supporting previous findings showing that the anterior cerebellum represents motor and premotor cortical networks (e.g., Buckner et al., 2011; O'Reilly et al., 2010; Marek et al., 2018). These findings suggest that young adults may recruit the cerebellum to a greater extent than older adults (on average) for the purposes of coordinating hand and eye movements during joystick use (cf. Miall et al., 2001) and integrating visual and somatosensory signals into stable motion-based representations (Rondi-Reig et al., 2014). This proposed construction of spatial representations from self-motion cues was supported by recent evidence showing that a hippocampo-cerebellar-centered network was involved in mediating the translations between self-motion and sequences of goal-directed actions (Babayan et al., 2017). Moreover, disruption of cerebellar Purkinje cell activity adversely affected the construction of hippocampal spatial representations from self-motion inputs from the cerebellum (Lefort et al., 2015; Rochefort et al., 2011). When older good performers were compared with older poor performers, higher activation in the posterior cerebellum coupled with higher prefrontal activations suggest that the former group preserved better executive and spatial processing functions (Eekers et al., 2018; Stoodley et al., 2012). This interpretation supports previous neuropsychological studies that showed greater involvement of the posterior cerebellum in executive and visuospatial functions than the anterior cerebellum, with lesions of the posterior lobe creating substantially greater declines in such functions compared with lesions of the anterior lobe (Schmahmann and Sherman, 1998; Schmahmann and Pandya, 1997). In addition, it is also possible that the relatively accurate search performance of older good performers was sustained by non-disruption to the neural circuits connecting the cerebellum to the prefrontal lobules (Schmahmann and Sherman, 1998; Schmahmann and Caplan, 2006).

Turning to the correlational results, search accuracy was found to correlate positively with activation in the lingual gyrus (BA 18), posterior cerebellum, precuneus (BA7), and premotor cortex (BA 6), across all participants. As noted above the involvement of the cerebellum and lingual gyrus play important roles in coordinating hand-eye coordination for directing successful goal-oriented search (Miall et al., 2001; Sherrill et al., 2015) while the involvement of fronto-parietal regions like the premotor cortex and the precuneus, may support updating and integrating egocentric spatial relationships/representations (Gramann et al., 2006, 2010; Sherrill et al., 2013; Wolbers et al., 2008). These full-sample correlational findings, however, were not reproduced when the participants were divided by age. Correlations specific to each age group showed that significant clusters of activations were found in the young only, suggesting that the search accuracy measure was more closely tied to between-subjects variability in BOLD responses among the young than among older adults.

Notwithstanding the absence of significant correlations within the older sample, higher anterior hippocampal activation was associated with greater search accuracy in the young. Interestingly, this finding paralleled the findings by Viard et al. (2011), which showed that anterior hippocampal activation (bilateral) in human subjects increased with closer proximity to a particular goal location. At the neuronal level, it is possible that higher hippocampal activation close to the goal reflected an elevated firing of hippocampal place cells clustered around the goal location (see, e.g., de Cothi and Spiers, 2017; Dupret et al., 2010; Hollup et al., 2001; Hok et al., 2007). This interpretation supports computational models proposing a gradient ascent of brain activity as one gets closer to the goal (Bilkey and Clearwater, 2005; Burgess and O'Keefe, 1996; Trullier and Meyer, 2000; see also Spiers et al., 2018, for an alternative gradient descent perspective). The absence of any hippocampal activation in older adults (based on both within-group and correlational analyses), combined with the presence of activations in the prefrontal cortex (based on within- and between-group analyses) support Moffat et al. (2006) proposal of a compensatory shift of spatial memory functions away from a dependence on the hippocampus toward a greater dependence on the prefrontal cortex. Specifically, among older good performers, activations in the dlPFC and the orbitofrontal cortex may represent compensatory shifts of spatial processing away from medial temporal circuits. Further supporting the presence of a potential hippocampus-to-prefrontal compensatory shift rather than a more universal negative effect of aging, is that older poor performers exhibited prefrontal activation in the right dlPFC but performed poorly across almost all place trials.

In summary, this study presented novel findings showing prominent prefrontal activations in vMWM performance in both young and older adults. Older good performers exhibited comparable performance as younger adults and displayed greater engagement of the orbitofrontal cortex when compared with older poor performers. Brain-behavior correlations further showed that only younger adults engaged the hippocampus, which might have reflected their greater monitoring or updating of spatial/Euclidean relationships than older adults during hidden

platform search. To our knowledge, the strengths of this study were entailed by the fact it was the *first* fMRI study that adopted an individual differences approach toward the analysis of vMWM performance in older adults by dividing them into two subgroups of good and poor performers. It was also the first fMRI study that followed a rodent-based and proximity-centered protocol, which offers the merit of facilitating a comparison of findings between MWM studies involving animal and human subjects, respectively. Notably, we introduced the use of CCProx – which heretofore was found to be the most sensitive measure in rodent MWM studies – to human virtual MWM analysis. Furthermore, we acknowledge that the small samples of older good and poor performers adults (after median-split) might have limited our ability to identify a wider range of significant brain activations. Therefore, we advise against an over-interpretation of the current fMRI findings based on between-group comparisons and recommend future studies examining performance-related patterns of brain activations in the elderly to recruit a larger sample to verify and extend our current findings. As older poor performers' poor performance and relatively low levels of cerebellar activations might have stemmed from certain difficulties or inexperience with handling the fMRI-compatible joystick, we further advise the design and implementation of more user-friendly control devices for older adults in future neuroimaging studies. Despite these limitations, the fact that relatively distinct patterns of brain activations were found in each of the three age/performance groups should not be eschewed – as they provided invaluable insights into how prefrontal- and hippocampus-dependent processes/functions could aid spatial memory formation in both young and older adults. We also regard our rodent-based MWM protocol as a potential great contributor to translational cognitive aging research involving both humans and animal models and recommend its continued use in further investigations on individual differences in spatial memory formation.

## Declarations of interest

None.

## Acknowledgements

This study was supported by National Institutes of Health, U.S.A., Grant K18 AG048706 and Oregon State University's Carlson College of Veterinary Medicine, U.S.A., Pilot Project funds awarded to Kathy R. Magnusson. It was partly based on the first author's Honors thesis, which was internally reviewed. We thank Nytavia Wallace (Radiologist and fMRI technologist, Center for Advanced Brain Imaging, Georgia Institute of Technology) for technical assistance with fMRI data collection. We also thank Matthew E. Swarts (Research Scientist, School of Architecture, Georgia Institute of Technology) for invaluable assistance in programming the data recording functions of the virtual Morris water maze.

## References

Andersson, J.L., Hutton, C., Ashburner, J., Turner, R., Friston, K., et al., 2001. Modeling geometric deformations in EPI time series. NeuroImage 13, 903–919.

Antonova, E., Parslow, D., Brammer, M., Dawson, G.R., Jackson, S.H., Morris, R.G., 2009. Age-related neural activity during allocentric spatial memory. Memory 17, 125–143. https://doi.org/10.1080/09658210802077348.

Antonova, E., Parslow, D., Brammer, M., Simmons, A., Williams, S., Dawson, G.R., Morris, R., 2011. Scopolamine disrupts hippocampal activity during allocentric spatial memory in humans: an fMRI study using a virtual reality analogue of the Morris water maze. J. Psychopharmacol. 25, 1256–1265. https://doi.org/10.1177/0269881110379285.

Astur, R.S., Ortiz, M.L., Sutherland, R.J., 1998. A characterization of performance by men and women in a virtual Morris water task: a large and reliable sex difference. Behav. Brain Res. 93, 185–190. https://doi.org/10.1016/S0166-4328(98)00019-9.

Astur, R.S., Taylor, L.B., Mamelak, A.N., Philpott, L., Sutherland, R.J., 2002. Humans with hippocampus damage display severe spatial memory impairments in a virtual Morris water task. Behav. Brain Res. 132, 77–84. https://doi.org/10.1016/S0166-4328(01)00399-0.

Babayan, B.M., Watilliaux, A., Viejo, G., Paradis, A.L., Girard, B., Rondi-Reig, L., 2017. A hippocampo-cerebellar centred network for the learning and execution of sequence-based navigation. Sci. Rep. 7, 17812. https://doi.org/10.1038/s41598-017-18004-7.

Barnes, C.A., Rao, G., Orr, G., 2000. Age-related decrease in the Schaffer collateral-evoked EPSP in awake, freely behaving rats. Neural Plast. 7, 167–178. https://doi.org/10.1155/NP.2000.167.

Bilkey, D.K., Clearwater, J.M., 2005. The dynamic nature of spatial encoding in the hippocampus. Behav. Neurosci. 119, 1533–1545. https://doi.org/10.1037/0735-7044.119.6.1533.

Blumenfeld, R.S., Parks, C.M., Yonelinas, A.P., Ranganath, C., 2011. Putting the pieces together: the role of dorsolateral prefrontal cortex in relational memory encoding. J. Cogn. Neurosci. 23, 257–265. https://doi.org/10.1162/jocn.2010.21459.

Brim, B.L., Haskell, R., Awedikian, R., Ellinwood, N.M., Jin, L., Kumar, A., Foster, T.C., Magnusson, K.R., 2013. Memory in aged mice is rescued by enhanced expression of the GluN2B subunit of the NMDA receptor. Behav. Brain Res. 238, 211–226. https://doi.org/10.1016/j.bbr.2012.10.026.

Buckner, R.L., Krienen, F.M., Castellanos, A., Diaz, J.C., Yeo, B.T., 2011. The organization of the human cerebellum estimated by intrinsic functional connectivity. J. Neurophysiol. 106, 2322–2345. https://doi.org/10.1152/jn.00339.2011.

Burgess, N., O'Keefe, J., 1996. Neuronal computations underlying the firing of place cells and their role in navigation. Hippocampus 6, 749–762. https://doi.org/10.1002/(SICI)1098-1063(1996)6:6%3c749::AID-HIPO16%3e3.0.CO;2-0.

Cabeza, R., 2001. Cognitive neuroscience of aging: contributions of functional neuroimaging. Scand. J. Psychol. 42, 277–286. https://doi.org/10.1111/1467-9450.00237.

Chen, G., Chen, K.S., Knox, J., Inglis, J., Bernard, A., Martin, S.J., Justice, A., McConlogue, L., Games, D., Freedman, S.B., Morris, R.G., 2000. A learning deficit related to age and beta-amyloid plaques in a mouse model of Alzheimer's disease. Nature 408, 975–979. https://doi.org/10.1038/35050103.

Chrastil, E.R., Sherrill, K.R., Aselcioglu, I., Hasselmo, M.E., Stern, C.E., 2017. Individual differences in human path integration abilities correlate with gray matter volume in retrosplenial cortex, Hippocampus, and medial prefrontal cortex. eNeuro 4. https://doi.org/10.1523/ENEURO.0346-16.2017.

Clark, A.S., Magnusson, K.R., Cotman, C.W., 1992. In vitro autoradiography of hippocampal excitatory amino acid binding in aged Fischer 344 rats: relationship to performance on the Morris water maze. Behav. Neurosci. 106, 324–335. https://doi.org/10.1037/0735-7044.106.2.324.

Curtis, C.E., D'Esposito, M., 2004. The effects of prefrontal lesions on working memory performance and theory. Cognit. Affect Behav. Neurosci. 4, 528–539. https://doi.org/10.3758/CABN.4.4.528.

Das, S.R., Magnusson, K.R., 2008. Relationship between mRNA expression of splice forms of the zeta1 subunit of the N-methyl-D-aspartate receptor and spatial memory in aged mice. Brain Res. 1207, 142–154. https://doi.org/10.1016/j.brainres.2008.02.046.

Das, S.R., Magnusson, K.R., 2011. Changes in expression of splice cassettes of NMDA receptor GluN1 subunits within the frontal lobe and memory in mice during aging. Behav. Brain Res. 222, 122–133. https://doi.org/10.1016/j.bbr.2011.03.045.

Das, S.R., Jensen, R., Kelsay, R., Shumaker, M., Bochart, R., Brim, B., Zamzow, D., Magnusson, K.R., 2012. Reducing expression of GluN1(0XX) subunit slice variants of the NMDA receptor interferes with spatial reference memory. Behav. Brain Res. 230, 317–324. https://doi.org/10.1016/j.bbr.2012.02.014.

Daugherty, A.M., Raz, N., 2017. A virtual water maze revisited: two-year changes in navigation performance and their neural correlates in healthy adults. Neuroimage 146, 492–506. https://doi.org/10.1016/j.neuroimage.2016.09.044.

Daugherty, A.M., Yuan, P., Dahle, C.L., Bender, A.R., Yang, Y., Raz, N., 2015. Path complexity in virtual water maze navigation: differential associations with age, sex, and regional brain volume. Cerebr. Cortex 25, 3122–3131. https://doi.org/10.1093/cercor/bhu107.

de Cothi, W., Spiers, H.J., 2017. Spatial cognition: goal-vector cells in the bat hippocampus. Curr. Biol. 27, R239–R241. https://doi.org/10.1016/j.cub.2017.01.061.

Domenech, P., Koechlin, E., 2015. Executive control and decision-making in the prefrontal cortex. Curr. Opin. Behav. Sci. 1, 101–106. https://doi.org/10.1016/j.cobeha.2014.10.007.

Driscoll, I., Hamilton, D.A., Petropoulos, H., Yeo, R.A., Brooks, W.M., Baumgartner, R.N., Sutherland, R.J., 2003. The aging hippocampus: cognitive, biochemical and structural findings. Cerebr. Cortex 13, 1344–1351.

Driscoll, I., Hamilton, D.A., Yeo, R.A., Brooks, W.M., Sutherland, R.J., 2005. Virtual navigation in humans: the impact of age, sex, and hormones on place learning. Horm. Behav. 47, 326–335. https://doi.org/10.1093/cercor/bhg081.

Driscoll, I., Hong, N.S., Craig, L.A., Sutherland, R.J., McDonald, R.J., 2008. Enhanced cell death and learning deficits after a mini-stroke in aged hippocampus. Neurobiol. Aging 29, 1847–1858. https://doi.org/10.1016/j.yhbeh.2004.11.013.

Driscoll, I., Howard, S.R., Stone, J.C., Monfils, M.H., Tomanek, B., Brooks, W.M., Sutherland, R.J., 2006. The aging hippocampus: a multi-level analysis in the rat. Neuroscience 139, 1173–1185. https://doi.org/10.1016/j.neuroscience.2006.01.040.

Dupret, D., O'Neill, J., Pleydell-Bouverie, B., Csicsvari, J., 2010. The reorganization and reactivation of hippocampal maps predict spatial memory performance. Nat. Neurosci. 13, 995–1002. https://doi.org/10.1038/nn.2599.

Eekers, D.B.P., In 't Ven, L., Deprez, S., Jacobi, L., Roelofs, E., Hoeben, A., Lambin, P., de Ruysscher, D., Troost, E.G.C., 2018. The posterior cerebellum, a new organ at risk? Clin. Transl. Radiat. Oncol. 8, 22–26. https://doi.org/10.1016/j.ctro.2017.11.010.

Folstein, M.F., Folstein, S.E., McHugh, P.R., 1975. Mini-mental state". A practical method for grading the cognitive state of patients for the clinician. J. Psychiatr. Res. 12, 189–198. https://doi.org/10.1016/0022-3956(75)90026-6.

Frey, S., Petrides, M., 2000. Orbitofrontal cortex: a key prefrontal region for encoding information. Proc. Natl. Acad. Sci. U.S.A. 97, 8723–8727. https://doi.org/10.1073/pnas.140543497.

Funahashi, S., 2017. Working memory in the prefrontal cortex. Brain Sci. 7. https://doi.org/10.3390/brainsci7050049.
Gallagher, M., Burwell, R., Burchinal, M., 1993. Severity of spatial learning impairment in aging: development of a learning index for performance in the Morris water maze. Behav. Neurosci. 107, 618–626. https://doi.org/10.1037/0735-7044.107.4.618.
Gallagher, M., Pelleymounter, M.A., 1988. Spatial learning deficits in old rats: a model for memory decline in the aged. Neurobiol. Aging 9, 549–556. https://doi.org/10.1016/S0197-4580(88)80112-X.
Grady, C.L., Maisog, J.M., Horwitz, B., Ungerleider, L.G., Mentis, M.J., Salerno, J.A., Pietrini, P., Wagner, E., Haxby, J.V., 1994. Age-related changes in cortical blood flow activation during visual processing of faces and location. J. Neurosci. 14, 1450–1462. https://doi.org/10.1523/JNEUROSCI.14-03-01450.1994.
Gramann, K., 2013. Embodiment of spatial reference frames and individual differences in reference frame proclivity. Spat. Cogn. Comput. 13, 1–25. https://doi.org/10.1080/13875868.2011.589038.
Gramann, K., Muller, H.J., Schonebeck, B., Debus, G., 2006. The neural basis of ego- and allocentric reference frames in spatial navigation: evidence from spatio-temporal coupled current density reconstruction. Brain Res. 1118, 116–129. https://doi.org/10.1016/j.brainres.2006.08.005.
Gramann, K., Onton, J., Riccobon, D., Mueller, H.J., Bardins, S., Makeig, S., 2010. Human brain dynamics accompanying use of egocentric and allocentric reference frames during navigation. J. Cogn. Neurosci. 22, 2836–2849. https://doi.org/10.1162/jocn.2009.21369.
Hok, V., Lenck-Santini, P.P., Roux, S., Save, E., Muller, R.U., Poucet, B., 2007. Goal-related activity in hippocampal place cells. J. Neurosci. 27, 472–482. https://doi.org/10.1523/JNEUROSCI.2864-06.2007.
Hollup, S.A., Molden, S., Donnett, J.G., Moser, M.B., Moser, E.I., 2001. Accumulation of hippocampal place fields at the goal location in an annular watermaze task. J. Neurosci. 21, 1635–1644. https://doi.org/10.1523/JNEUROSCI.21-05-01635.2001.
Iaria, G., Chen, J.K., Guariglia, C., Ptito, A., Petrides, M., 2007. Retrosplenial and hippocampal brain regions in human navigation: complementary functional contributions to the formation and use of cognitive maps. Eur. J. Neurosci. 25, 890–899. https://doi.org/10.1111/j.1460-9568.2007.05371.
Korthauer, L.E., Nowak, N.T., Moffat, S.D., An, Y., Rowland, L.M., Barker, P.B., Resnick, S.M., Driscoll, I., 2016. Correlates of virtual navigation performance in older adults. Neurobiol. Aging 39, 118–127. https://doi.org/10.1016/j.neurobiolaging.2015.12.003.
Kringelbach, M.L., Rolls, E.T., 2004. The functional neuroanatomy of the human orbitofrontal cortex: evidence from neuroimaging and neuropsychology. Prog. Neurobiol. 72, 341–372. https://doi.org/10.1016/j.pneurobio.2004.03.006.
Lefort, J.M., Rochefort, C., Rondi-Reig, L., 2015. Cerebellar contribution to spatial navigation: new insights into potential mechanisms. Cerebellum 14, 59–62. https://doi.org/10.1007/s12311-015-0653-0.
Lester, A.W., Moffat, S.D., Wiener, J.M., Barnes, C.A., Wolbers, T., 2017. The aging navigational system. Neuron 95, 1019–1035. https://doi.org/10.1016/j.neuron.2017.06.037.
Maei, H.R., Zaslavsky, K., Teixeira, C.M., Frankland, P.W., 2009. What is the most sensitive measure of water maze probe test performance? Front. Integr. Neurosci. 3, 4. https://doi.org/10.3389/neuro.07.004.2009.
Magnusson, K.R., 1998. Aging of glutamate receptors: correlations between binding and spatial memory performance in mice. Mech. Ageing Dev. 104, 227–248. https://doi.org/10.1016/S0047-6374(98)00076-1.
Magnusson, K.R., 2001. Influence of diet restriction on NMDA receptor subunits and learning during aging. Neurobiol. Aging 22, 613–627. https://doi.org/10.1016/S0187-4580(00)00258-X.
Magnusson, K.R., Scruggs, B., Zhao, X., Hammersmark, R., 2007. Age-related declines in a two-day reference memory task are associated with changes in NMDA receptor subunits in mice. BMC Neurosci. 8, 43. https://doi.org/10.1186/1471-2202-8-43.
Marek, S., Siegel, J.S., Gordon, E.M., Raut, R.V., Gratton, C., Newbold, D.J., Ortega, M., Laumann, T.O., Adeyemo, B., Miller, D.B., Zheng, A., Lopez, K.C., Berg, J.J., Coalson, R.S., Nguyen, A.L., Dierker, D., Van, A.N., Hoyt, C.R., McDermott, K.B., Norris, S.A., Shimony, J.S., Snyder, A.Z., Nelson, S.M., Barch, D.M., Schlaggar, B.L., Raichle, M.E., Petersen, S.E., Greene, D.J., Dosenbach, N.U.F., 2018. Spatial and temporal organization of the individual human cerebellum. Neuron 100, 977–993 e977. https://doi.org/10.2139/ssrn.3188429.
Miall, R.C., Reckess, G.Z., Imamizu, H., 2001. The cerebellum coordinates eye and hand tracking movements. Nat. Neurosci. 4, 638–644. https://doi.org/10.1038/88465.
Moffat, S.D., Elkins, W., Resnick, S.M., 2006. Age differences in the neural systems supporting human allocentric spatial navigation. Neurobiol. Aging 27, 965–972. https://doi.org/10.1016/j.neurobiolaging.2005.05.011.
Moffat, S.D., Kennedy, K.M., Rodrigue, K.M., Raz, N., 2007. Extrahippocampal contributions to age differences in human spatial navigation. Cerebr. Cortex 17, 1274–1282. https://doi.org/10.1093/cercor/bhl036.
Moffat, S.D., Resnick, S.M., 2002. Effects of age on virtual environment place navigation and allocentric cognitive mapping. Behav. Neurosci. 116, 851–859. https://doi.org/10.1037/0735-7044.116.5.851.
Morris, R., 1981. Spatial localization does not require the presence of local cues. Learn. Motive 12, 239–260. https://doi.org/10.1016/0023-9690(81)90020-5.
Morris, R., 1984. Developments of a water-maze procedure for studying spatial learning in the rat. J. Neurosci. Methods 11, 47–60. https://doi.org/10.1016/0165-0270(84)90007-4.
Nowak, N.T., Diamond, M.P., Land, S.J., Moffat, S.D., 2014. Contributions of sex, testosterone, and androgen receptor CAG repeat number to virtual Morris water maze performance. Psychoneuroendocrinology 41, 13–22. https://doi.org/10.1016/j.psyneuen.2013.12.003.
O'Bryant, S.E., Humphreys, J.D., Smith, G.E., Ivnik, R.J., Graff-Radford, N.R., Petersen, R.C., Lucas, J.A., 2008. Detecting dementia with the mini-mental state examination in highly educated individuals. Arch. Neurol. 65, 963–967. https://doi.org/10.1001/archneur.65.7.963.
O'Reilly, J.X., Beckmann, C.F., Tomassini, V., Ramnani, N., Johansen-Berg, H., 2010. Distinct and overlapping functional zones in the cerebellum defined by resting state functional connectivity. Cerebr. Cortex 20, 953–965. https://doi.org/10.1093/cercor/bhp157.
Oldfield, R.C., 1971. The assessment and analysis of handedness: the Edinburgh inventory. Neuropsychologia 9, 97–113. https://doi.org/10.1016/0028-3932(71)90067-4.
Ongür, D., Ferry, A.T., Price, J.L., 2003. Architectonic subdivision of the human orbital and medial prefrontal cortex. J. Comp. Neurol. 460, 425–449. https://doi.org/10.1002/cne.10609.
Radloff, L.S., 1977. The CES-D scale: a self-report depression scale for research in the general population. Appl. Psychol. Meas. 1, 385–401. https://doi.org/10.1177/014662167700100306.
Ramnani, N., Owen, A.M., 2004. Anterior prefrontal cortex: insights into function from anatomy and neuroimaging. Nat. Rev. Neurosci. 5, 184–194. https://doi.org/10.1038/nrn1343.
Reuter-Lorenz, P.A., Cappell, K.A., 2008. Neurocognitive aging and the compensation hypothesis. Curr. Dir. Psychol. Sci. 17, 177–182. https://doi.org/10.1111/j.1467-8721.2008.00570.
Rochefort, C., Arabo, A., André, M., Poucet, B., Save, E., Rondi-Reig, L., 2011. Cerebellum shapes hippocampal spatial code. Science 334, 385–389. https://doi.org/10.1126/science.1207403.
Rondi-Reig, L., Paradis, A.L., Lefort, J.M., Babayan, B.M., Tobin, C., 2014. How the cerebellum may monitor sensory information for spatial representation. Front. Syst. Neurosci. 8, 205. https://doi.org/10.3389/fnsys.2014.00205.
Schmahmann, J.D., Caplan, D., 2006. Cognition, emotion and the cerebellum. Brain 129, 290–292. https://doi.org/10.1093/brain/awh729.
Schmahmann, J.D., Pandya, D.N., 1997. The cerebrocerebellar system. Int. Rev. Neurobiol. 41, 31–60. https://doi.org/10.1016/S0074-7742(08)60346-3.
Schmahmann, J.D., Sherman, J.C., 1998. The cerebellar cognitive affective syndrome. Brain 121, 561–579. https://doi.org/10.1093/brain/121.4.561.
Sherrill, K.R., Chrastil, E.R., Ross, R.S., Erdem, U.M., Hasselmo, M.E., Stern, C.E., 2015. Functional connections between optic flow areas and navigationally responsive brain regions during goal-directed navigation. Neuroimage 118, 386–396. https://doi.org/10.1016/j.neuroimage.2015.06.009.
Sherrill, K.R., Erdem, U.M., Ross, R.S., Brown, T.I., Hasselmo, M.E., Stern, C.E., 2013. Hippocampus and retrosplenial cortex combine path integration signals for successful navigation. J. Neurosci. 33, 19304–19313. https://doi.org/10.1523/JNEUROSCI.1825-13.2013.
Shine, J.P., Valdes-Herrera, J.P., Hegarty, M., Wolbers, T., 2016. The human retrosplenial cortex and thalamus code head direction in a global reference frame. J. Neurosci. 36, 6371–6381. https://doi.org/10.1523/JNEUROSCI.1268-15.2016.
Slotnick, S.D., Moo, L.R., 2006. Prefrontal cortex hemispheric specialization for categorical and coordinate visual spatial memory. Neuropsychologia 44, 1560–1568. https://doi.org/10.1016/j.neuropsychologia.2006.01.018.
Spiers, H.J., 2008. Keeping the goal in mind: prefrontal contributions to spatial navigation. Neuropsychologia 46, 2106–2108.
Spiers, H.J., Maguire, E.A., 2006. Thoughts, behaviour, and brain dynamics during navigation in the real world. Neuroimage 31, 1826–1840. https://doi.org/10.1016/j.neuropsychologia.2008.01.028.
Spiers, H.J., Maguire, E.A., 2007. A navigational guidance system in the human brain. Hippocampus 17, 618–626. https://doi.org/10.1016/j.neuroimage.2006.01.037.
Spiers, H.J., Olafsdottir, H.F., Lever, C., 2018. Hippocampal CA1 activity correlated with the distance to the goal and navigation performance. Hippocampus 28, 644–658. https://doi.org/10.1002/hipo.22813.
Stoodley, C.J., Valera, E.M., Schmahmann, J.D., 2012. Functional topography of the cerebellum for motor and cognitive tasks: an fMRI study. Neuroimage 59, 1560–1570. https://doi.org/10.1016/j.neuroimage.2011.08.065.
Sutherland, R.J., Dyck, R.H., 1984. Place navigation by rats in a swimming pool. Can. J. Psychol. 38, 322–347. https://doi.org/10.1037/h0080832.
Trullier, O., Meyer, J.A., 2000. Animat navigation using a cognitive graph. Biol. Cybern. 83, 271–285. https://doi.org/10.1007/s004220000170.
van Praag, H., Shubert, T., Zhao, C., Gage, F.H., 2005. Exercise enhances learning and hippocampal neurogenesis in aged mice. J. Neurosci. 25, 8680–8685. https://doi.org/10.1523/JNEUROSCI.1731-05.2005.
Viard, A., Doeller, C.F., Hartley, T., Bird, C.M., Burgess, N., 2011. Anterior hippocampus and goal-directed spatial decision making. J. Neurosci. 31, 4613–4621. https://doi.org/10.1523/JNEUROSCI.4640-10.2011.
Wolbers, T., Hegarty, M., Buchel, C., Loomis, J.M., 2008. Spatial updating: how the brain keeps track of changing object locations during observer motion. Nat. Neurosci. 11, 1223–1230. https://doi.org/10.1038/nn.2189.
Yuan, P., Daugherty, A.M., Raz, N., 2014. Turning bias in virtual spatial navigation: age-related differences and neuroanatomical correlates. Biol. Psychol. 96, 8–19. https://doi.org/10.1016/j.biopsycho.2013.10.009.
Zamzow, D.R., Elias, V., Acosta, V.A., Escobedo, E., Magnusson, K.R., 2016. Higher levels of phosphorylated Y1472 on GluN2B subunits in the frontal cortex of aged mice are associated with good spatial reference memory, but not cognitive flexibility. Age (Dordr). 38, 50. https://doi.org/10.1007/s11357-016-9913-2.
Zamzow, D.R., Elias, V., Acosta, V.A., Escobedo, E., Magnusson, K.R., 2019. Higher levels of protein palmitoylation in the frontal cortex across aging were associated with reference memory and executive function declines. eNeuro 6. https://doi.org/10.1523/ENEURO.0310-18.2019.

Zhao, X., Rosenke, R., Kronemann, D., Brim, B., Das, S.R., Dunah, A.W., Magnusson, K.R., 2009. The effects of aging on N-methyl-D-aspartate receptor subunits in the synaptic membrane and relationships to long-term spatial memory. Neuroscience 162, 933–945. https://doi.org/10.1016/j.neuroscience.2009.05.018.

Zhong, J.Y., 2016. What does neuroscience research tellus about human consciousness? An overview of Benjamin Libet's legacy. J. Mind Behav. 37, 287–309.

Zhong, J.Y., Magnusson, K.R., Swarts, M.E., Clendinen, C.A., Reynolds, N.C., Moffat, S.D., 2017. The application of a rodent-based Morris water maze (MWM) protocol to an investigation of age-related differences in human spatial learning. Behav. Neurosci. 131, 470–482. https://doi.org/10.1037/bne0000219.

Zhong, J.Y., Moffat, S.D., 2018. Extrahippocampal contributions to age-related changes in spatial navigation ability. Front. Hum. Neurosci. 12, 272. https://doi.org/10.3389/fnhum.2018.00272.